Detection of polystryrene nanoplastics in biological samples based on the solvatochromic properties of Nile Red: application in *Hydra attenuata* exposed to nanoplastics.

François Gagné[1], Joëlle Auclair[1], Brian Quinn[2].

[1] Aquatic Contaminant Research Division, Environment and Climate Change Canada, Montreal, Quebec, Canada.

[2] School of Health and Life Sciences, University of the West of Scotland, Paisley PA1 2BE, Scotland, United Kingdom

Abstract

The release of nanoplastics (NP) from the weathering of microplastics is a major concern for the environment. Methods for the detection of NP in biological tissues are urgently needed because of their ability to penetrate not only in tissues but in cells. A simple fluorescence-based methodology for the detection of polystyrene NP in biological tissues is proposed using the solvatochromic probe Nile Red. NPs were found to display autofluorescence at 460 and 665-700 nm during excitation at 400 nm. Although NPs alone increased somewhat Nile red fluorescence, a characteristic hypsochromic shift in the emission spectra was found when the dye and NP were incubated with subcellular tissue fraction. To explain this, the probe and NPs (50 and 100 nm) were prepared in the presence of increasing concentrations of two detergents (Tween-20, Triton X100) as a proxy to phospholipids. The data revealed that both detergents readily increased fluorescence values when added to the NP and Nile red. The addition of NPs in tissue extracts blue shifted further the emission spectra to 623 nm from the normal Nile Red-lipid peak at 660 nm. The fluorescence intensity was proportional to the NP concentration. A methodology is thus proposed for the detection of NPs in laboratory-exposed organisms based on the solvatochromic properties of Nile red. The methodology was used to detect the presence of NP and changes in polar lipid contents in *Hydra attenuata* exposed to polystyrene NP.

Key words: polystyrene, nanoplastic, Nile Red, fluorescence, detection.

Contact information: francois.gagne@canada.ca

Introduction

The increase in plastic pollution of the oceans and freshwater bodies has raised concerns for their possible environment impacts. Pollution of the oceans by plastic material has been raised as early in the 1970s (Carpenter and Smith, 1972) and reached important proportions some 50 years latter. Microplastics are operationally defined as particles between 5 mm to 1 µm while NP are between 1-1000 nm in size (Gigault et al., 2016). Microplastic materials were detected in water, sediments and organisms (Browne et al., 2011, vanSebile, 2014). Small bits of plastics could be ingested by

organisms and find their way through the food chain including humans (Smith et al., 2018). In a large-scale survey with the freshwater Asian clam, the concentrations of microplastics ranged from 0.3 – 5 items per individual clams, 0.5-3 items/L in water and 15-160 items in sediments (Su et al., 2018). Invertebrates can be exposed to microplastic contamination given their capacity to feed on suspended material in the water column and particles at the sediment-water interface (Murphy and Quinn, 2018; Magni et al., 2018). In another study, clams were exposed to 1 mg/L (20 µm) polyethylene microplastic for 14 days, was accumulated in tissues and were difficult to eliminate by depuration (Ribeiro et al., 2017). This resulted led to oxidative damage, DNA damage and neurotoxicity.

Contamination of organisms with microplastics is considered the "tip of the iceberg" problem given that most plastics will persist for a long time and subject to degradation in the environment. Microplastics are expected to degrade by weathering processes which will release, in turn, very high quantities of nanoplastics (NP) in the environment (Lambert and Wagner, 2016; daCosta et al., 2016). To highlight this, a recent study revealed that degradation of a polystyrene coffee cup lid liberated nanoparticles in the order of $1.3x10^8$ particles with a mean particle size of 224 nm after 56 days. At this scale, NP behave as colloids i.e., will disperse in water and may increase exposure to aquatic fauna and flora. In addition, NPs are not only bioavailable in tissues but at the subcellular/macromolecular level as often observed with other nanoparticles (Lovric et al., 2005). Although plastics in the environment could be considered as biochemically inert in organisms (Magni et al., 2018), recent evidence suggest that NPs could have some emerging properties at the nanoscale such as increasing hydrophobic interactions leading to protein conformational changes as seen with polyamidoamine dendrimers (Auclair et al., 2017) and some redox properties with

small polyethylene microplastics (Gagné et al., 2018). Hence, the urgent need to have methods at hand to enable their detection in biological tissues/cells.

Nile red (NR) is a fluorescent probe that detects hydrophobic environments and is currently used as a stain for lipid droplets in cells (Greenspan et al, 1985) and for microplastic detection using epifluorescence microscopy (Erni-Cassola et al., 2017). NR is soluble in water and its fluorescence is greatly enhanced in the presence of hydrophobic agents (lipids) but not by proteins when excitated at 400-500 nm. The NR staining method was able to stain different types of plastics such as polyethylene, polypropylene, polystyrene, polycarbonate, polyurethane and poly(ethylene-vinyl acetate) but does not work for polyvinylchloride, polyamide and polyester (Shim et al., 2016). In addition to the increased fluorescence, the emission maxima undergo a hypsochromic shift (blue shift) as the environment becomes more hydrophobic. For example, the emission spectra is shifted to shorter wavelength as the polarity decreases: from 620 nm in acetone to 520 nm in n-heptane. NR is also used to detect microplastics as it binds to plastic particles and could be observed by epifluorescence microscopy (Maes et al., 2017). Microplastic particles are isolated from water and sediment by density-based gradient extraction where they tend to float to the surface in high salt solution (Quinn et al., 2016). The microplastic particles are then isolated on filter paper, stained by NR and viewed/counted by microscopy. Positive identification is followed using the standard Fourier-transform infrared microscopy technique. Although this approach is very convenient to detect microplastics, the method does not work nanoplastics (NP) of size below of 0.1 µm since they are not observable by photon microscopy. Although NP could be detected by electron microscopy, the approach is not quantitative and a rapid and simple methodology for NP detection in tissues would be of value. Since NP could pass to the intracellular environment as often observed with other nanomaterials (Lovric et al., 2005), the development of methods to detect their

occurrence in tissues/cells is urgently needed. Recently, 2 other methods were proposed to detect polystyrene NPs in tissues which makes use of molecular rotor and fluorescence polarisation probes (Gagné, 2019; Gagné et al., 2019). However they do not provide the additional lipid measurement with NR which could provide additional effects of NP-induced effects at the subcellular levels. It is hypothetized that the hydrophobic nature of NP introduce hydrophobic interactions in the intracellular media given their high surface area/volume ratio which could be sensed by solvatochromic dyes such as NR. The purpose of this study was to determine whether changes in NR fluorescence in invertebrates (mussel and Hydra) tissues could be used to detect for the presence of polystyrene NP in addition to lipid droplets. A method is proposed for the semi-quantitative detection of NP in biological tissues in organisms exposed to polystyrene NPs.

Methods

Reagents and tissue preparation

Triton X-100, tween-20, dimethylsulfoxide (DMSO), methanol, Nile Red (NR; 9-diethylamino-5-benzo[*a*]phenoxazinone) were purchased from Sigma chemical company (ON, Canada). Uncoated polystyrene plastic nanobeads of 100 and 50 nm diameter were purchased from Polyscience (USA). The validation of the methodology was performed using subcellular extracts of digestive gland of freshwater mussels *Elliptio complanata* because of the higher quantities of tissues than in Hydra and the eventual application to bivalves exposed to NPs given the recent literature data. The developed methodology was applied on *Hydra attenuata* exposed to NPs for 96 h was described below. The tissue extracts were prepared from freshwater mussels (*Elliptio complanata*) as follows. Adult mussels (76±6 mm shell length) were dissected on ice for the digestive gland and homogenized at 20% (w/v) in ice-cold 100 mM NaCl containing 25 mM Hepes-NaOH, pH 7.4, 0.1 mM dithiothreitol and 1 ug/mL apoprotinin. The homogenate was centrifuged at 15 000 x g

for 20 min at 2°C. The resulting supernatant (S15 fraction) were collected from the pellet and upper lipid layer and stored at -85°C until analysis. This fraction was named the subcellular fraction in the text. The NP suspensions did not precipitate at this centrifugation speed and freezing at -85°C did not produce any precipitation after thawing and centrifugation. The subcellular fraction of the digestive gland from 3 individuals were pooled for fluorescence studies. Total proteins were determined using the protein dye binding potential (Bradford, 1976). Briefly, the assay run in clear 96-well microplates, with 10 uL of diluted homogenate or subcellular fraction was mixed with 150 µL of water and 40 µL of the Coomassie blue G250 dye reagent. After mixing, the absorbance at 590 nm was measured using a microplate reader (Synergy-4, Biotek Instruments, USA). Standard solutions of serum bovine albumin (2-10 µg/mL) were used for calibration.

Fluorescence analysis of NPs

The stock solution of NR was prepared in methanol at 1 mM and stored in the dark at 4°C. The NR probe was diluted at 10 µM in MilliQ water just before the fluorescence assays. A sample volume of 50 µL of increasing concentration of NP (final concentration: 0, 0.1, 0.2, 0.4 and 0.8 µg/mL) in water or in the presence of the subcellular fraction (0.15 mg/mL total protein) was mixed with 200 µL of 10 µM NR probe for 10 min in dark 96-well microplates. The emission spectra between 530-800 nm was obtained at 500 nm excitation using a microplate fluorimeter (Synergy-4, Biotek, USA). To determine the influence of detergents (analoguous to phospholipids) on the observed emission signals, the probe (200 µL) was mixed with increasing concentrations of triton X-100 and tween-20 (50µL sample volume) between 0.2-0.8 µg/mL. The detergent tween-20 was heavier and denser ($C_{58}H_{114}O_{26}$, MW=1227 g/mol, 1.12 g/mL) than triton X-100 ($C_{14}H_{22}O(C_2H_4O)_{9\text{-}10}$, 624 g/mol, 1.07 g/mL) thus providing more hydrophobic interactions.

125 ***Hydra exposure to NP***

126 *Hydra attenuata* were exposed to 50 nm polystyrene NP following a previously described
127 methodology (Blaise et al., 2018 and supplementary file). Briefly, the Hydra were cultured in 20-
128 cm diameter crystallisation bowls at room temperature in the incubation medium: 1 mM $CaCl_2$
129 and 0.5 mM TES buffer, pH 7.0. Three individuals were placed in each 12-well (N=3x3 Hydra per
130 exposure concentration) microplates and exposed to increasing concentrations of 50 nm
131 polystyrene NP: 0, 1.25, 5, 10, 20, 40 and 80 mg/L for 96-h at 20^{o}C. After the exposure period,
132 The hydra were rinced once with the hydra culture medium: 1 mM $CaCl_2$ and 0.5 mM TES buffer,
133 pH 7.0 and homogenized in 50mM NaCl, 25mM Hepes 0.1mM dithiothreitol pH 7.4. A 100 µL
134 of the homogenate was mixed with 25 µL of 10 µM NR dye for 15 min and analyzed for
135 fluorescence at 500 nm excitation and emission between 530-800 nm. The fluorescence intensity
136 at 660 and 623 nm was taken for polar lipids (Luo et al., 2009) and NP accumulation assessments
137 respectively. Fluorescence data were expressed as relative fluorescence units (RFU)/Hydra. In a
138 parallel experiment, Hydra were exposed to fluorescein-labeled polystryrene NPs of the same size
139 (Polyscience, USA) in the same conditions as described above to confirm the availability of
140 fluorescently-labeled NP and correlation with transparent polystyrene NP as determined by the
141 present methodology (supplementary file). At the end of the exposure period, hydra were collected,
142 washed in culture media and homogenized as above. The level of fluorescein was measured at 485
143 nm excitation and 520 nm emission. The data are presented in the supplementary material (Fig
144 S1).

145 ***Data analysis***

146 Spectra scans data were obtained from the Synergy-4 microplate reader operating software
147 (Biotek, USA), imported to an Excell spreadsheet and analysed with SYSTAT software (version

13.2; USA). Fluorescence analyses were performed in triplicates samples for method development and the exposure experiments of Hydra to NPs were performed in triplicates. The theoretical limit of detection was defined as the concentration that produced a fluorescence signal corresponding to twice the standard deviation of the NR blank. The data were analysed by regression analysis and the least square method. Data significance were verified by analyse of variance (ANOVA) following Dunnett's t test. Significance was set at $p<0.05$.

Results

The fluorescence properties of polystyrene NPs in the presence of the solvatochromic dye NR were determined in the subcellular extract. The emission spectra of NR (excitation at 500 nm and emission between 530-800 nm) in the presence of increasing concentrations of NP in a fixed amount of subcellular extract (0.1 mg/mL) produced a concentration-dependent increase in fluorescence. In the presence of subcellular extract alone, the emission maxima was at 660 nm. The addition of 50 nm NP (Figure 1A) and 100 nm (Figure 1B) blue-shifted the spectra forming a characteristic shoulder in the emission spectra. Indeed, the emission intensity ratio at 623 nm/660 nm was increased from 0.86 to 1.20 when NP was added in the presence subcellular fraction. The first derivative of the fluorescence spectra of the 50 nm NPs in the subcellular fraction is shown which confirmed the fluorescence peak at 623 nm which differed from the subcellular fraction alone (Figure 1C). The emission intensity at 623 nm and 660 nm were determined with increasing concentrations of 50 and 100 nm NPs with a fixed amount of subcellular fraction (Figures 2A and 2B). The analysis revealed that the emission intensity at 623 nm increased linearly with 50 nm ($r=0.95$; $p<0.01$) and 100 nm ($r=0.91$; $p<0.01$) NPs which suggests that NPs could be semi-quantitatively detected in the presence of NR which is usually used to quantify lipids in intracellular environments. Interestingly, the addition of NP did increase somewhat the emission

171 at 660 nm for polar lipids suggesting that NP could also interfere in the determination of polar
172 lipids. This could be mitigated by using an analysis of covariance (with the polar lipids as the
173 covariate) as a mean of correction when testing for the presence of NPs in tissues. Another option
174 would be to extract the residuals of polar lipids if a significant correlation exists between emission
175 at 623 and 660 nm. Hence, given the spectral overlap between polar lipids at 660 nm and NP-
176 induced fluorescence at 623 nm, the method is thus considered semi-quantitative at best. In
177 situations were the 623/660 ratio > 1.1, this provides an indication of the presence of polystyrene
178 NP in tissues.

179 In the attempt to understand NR emission changes with NP when subcellular fraction is added, we
180 examined the emission spectra of a fixed amount of either 50 nm or 100 nm NP and NR dye (1
181 µg/mL) with increasing concentrations of 2 detergents differing in molecular weight and density
182 (Figure 3). In the case of triton X100, increasing its concentration lead to the concentration
183 dependent increase in emission at 640 nm with a fixed 50 nm NP concentration of 1 µg/mL in
184 water (no other lipids were present) (Figure 3A). With the 100 nm NP, the emission maxima was
185 at 654 nm in the presence of increasing concentration of triton X100. In the case of the heavier and
186 denser detergent tween-20, a concentration dependent increase of emission maximum at 633 nm
187 was obtained with this detergent at a fixed concentration of 1 µg/mL of 50 nm NP. The emission
188 maxima was shifted again at 627 nm with the 100 nm NP in a concentration dependant manner.
189 On the whole the data suggest that both the size of the NP and the nature (hydrophobicity) of the
190 detergent influenced the emission spectra of NR. Indeed, the higher molecular weight, viscous and
191 dense detergent tween-20 (1227 g/mol; 330 mPa.sec; 1.12g/mL) (Figures 3C and 3D) produced
192 emission spectra at lower wavelength than the detergent triton X100 (624 g/mol; 280 mPa.sec;

1.07g/mL) which suggests less polar interactions (Figures 3A and 3B). The 50 nm NP produced stronger emission spectra (increase quantum yield) than the 100 nm NPs for both detergents.

The NR methodology was tested with Hydra exposed to increasing concentrations of 50 nm polystyrene NP for 96 h (Figure 4). Polar lipid contents were determined at 660 nm and NP at 623 nm based on the above observations. The emission ratio at 623/660 was significantly increased (ANOVA $p<0.05$, Fisher Least Square $p=0.02$) in Hydra exposed to 50 nm polystyrene NP at $\geq$ 2.5 mg/L suggesting the presence of NP in Hydra homogenates. The fluorescence at 623 nm was significantly increased at NP concentrations $\geq$ 20 mg/L and the fluorescence at 660 nm for lipids were increased at 80 mg/L 50 nm NP. In a separate experiment, hydra were exposed to fluorescein-labeled polystyrene NP of the same size and revealed a similar uptake in NP (Figure S1, supplementary material). Moreover, the fluorescence at 623 nm (Nile red; unlabelled NP) was significantly correlated ($r=0.6$; $p<0.01$; supplementary data) with the levels of fluorescein-labelled NP 50 nm in Hydra.

Discussion

The excitation and emission spectra of NR shifted to shorter wavelength as the polarity of the solvent decreased which makes NR an efficient dye for the detection of hydrophobic material in cellular extracts (Greenspan and Fowler, 1985). Indeed, the emission maxima could shift from 650 nm in ethanol to 530 nm in iso-octane which makes this probe an efficient hydrophobicity sensor. It is also used as a dye to detect lipid vesicles and droplets in cells (Greenspan et al., 1985). In the presence of NP alone, the dye produce low fluorescence (Figure 2) but when lipids (from the subcellular fraction) or detergents were added with the NP, a characteristic blue shift of the

emission spectra in respect to polar lipids was observed. This suggests that the polystyrene NP produce hydrophobic environment than the normal lipid vesicles found in the subcellular extract. Polystyrene is composed of styrene (propylene-benzene) repeats considered of low polarity compared to charged fatty acids and phospholipids. Lipids could also adhere at the surface of the NP and produce a more hydrophobic environment than vesicles composed of polar phospholipids. The emission maxima of NP in the subcellular extract at 623 nm was somewhat lower than the emission maxima of NP prepared in tween-20 detergent which yielded an emission maxima at 627 nm for the 100 nm NP. When the NR dye were dispersed in phophatidylcholine or microsome membrane vesicles (which are present in the subcellular extract), the emission maxima was at 628 nm with an excitation at 549 nm and was blue shifted to 575-600 nm when neutral lipids such as triacylglycerol was added *in vitro* (Greenspan and Fowler, 1985). The emission ratio at 623/660 could serve as a means to detect hydrophobic changes by polystyrene NP in biological samples while determining polar lipids in cells at the same time. The theoretical limit of detection of 50 and 100 nm polystyrene NP was estimated at 0.1 µg/ml (2.5 ng total) and 0.3 µg/ml (7.5 ng) respectively. More research is needed to find other hydrophobic-sensitive fluorescence probes that provides better spectral resolution when NPs are present in the subcellular fraction. Again, because of spectral overlaps between lipids and NPs, the increase in NPs at 623 nm should be used to detect plastics at this scale in a semi-quantitative way i.e., should be considered as detection test for NP and not a definitive assay for NPs. Recent studies with other fluorescent dyes (molecular rotor and fluorescent polarization lipophilic probes) were also shown to detect NPs in tissues although they do not provide information on lipid contents (Gagné, 2019; Gagné et al., 2019). Indeed, the molecular rotor probe using 9-(dicyanovinyl)julolidine probe revealed that 50 nm and 100 nm polystyrene NPs could be directly measured in tissues and was in agreement with the present Nile

red methodology. In another study, the same NPs also induced anisotropic changes in tissues spiked with NPs. Evidence of NPs in the digestive gland of mussels exposed to municipal effluents was found which was measured by fluorescence polarization of fluorescein octadecyl ester probe (Gagné et al., 2019) and was also in agreement with the present NR methodology. The proposed Nile red methodology was in agreement with other assays for polystyrene NPs using molecular rotor and fluorescence polarization probes but has the advantage to detect polar and neutral lipid contents.

Exposure of polystyrene NPs in Hydra led to increase accumulation of NPs and increased polar lipid as determined by the emission at 623 and 660 nm respectively. The increase of lipids was observed by a number of compounds including nanoparticles and plasticizers. Exposure to zinc oxide nanoparticles in the yeast *Saccharomyces cerevisiae* led to cell death which was followed by stress responses involving in lipid dysregulation and proteostasis such as increased heat shock proteins, unfolded protein response (cytosolic Hac1 splicing) and induction in lipid droplets with distorted vacuolar morphology (Babele et al., 2018). In another study, exposure of *Daphnia geleata* polystyrene nanoplastics (52 nm) lead to mortality at 5 mg/L after 5 days (Cui et al., 2017). Although the adults showed decreased lipid droplets storage, the embryos displayed increased lipid droplets, which suggests decreased energy mobilization leading to very low hatching rates. A recent study identified a number of compounds that could alter fat storage in *Daphnia magna* that involved endocrine disruption (Jordao et al.. 2016). The antifouling compound tributytin activated the ecdysteroid juvenile hormone and retinoic X receptor signalling pathways leading to impaired transfer of triacylglycerol to eggs leading to lipid droplet accumulation in females. Other compounds producing similar effects (increased NR staining) included bisphenol A (found in some plastics), methy farnesoate, pyriproxifen (arthropod insecticide) and 20-hydroxyecdysone (the

moulting hormone in microcrustaceans). The lipid droplets were enriched in cholesterol and triacylglycerols at the expense of glycerophospholipids in female daphnids exposed to the juvenoids pyriproxyfen and methyl farnesoate (Fuertes et al,. 2018). *Daphnia magna* feeding activity was reduced by 100 nm polystyrene NP and was retained for longer times in tissues compared to 2 µm microplastics although no effect on reproduction was observed after 24 h exposure (Rist et al., 2017).

In conclusion, the solvatochromic NR probe used for the quantification of lipids in cells could be used to detect the presence of 50 and 100 nm transparent polystyrene NP. The characteristic changes in NR fluorescence suggests that NP introduce more hydrophobic interactions in the intracellular domain in cells compared to lipid vesicles in the cytoplasm. The toxic outcome of this phenomenon is still unknown at present and more studies are needed to better understand the influence of NPs on the mobilization of energy from lipids. The increase in polar lipids observed in Hydra exposed to 50 nm polystyrene NPs suggests that polystyrene NP could have an obesogen effect.

Acknowledgements

This work was funded through the Saint-Lawrence Action Plan of Environment and Climate Change Canada. The authors thank Pascale Bouchard for performing the hydra exposure assay.

Conflict of interest statement

The authors declare no conflict of interest in the submission process and financial influence on the research presented.

References

Auclair J, Morel E, Wilkinson KJ, Gagné F. Sublethal effects of poly-(amidoamine) dendrimers in rainbow trout hepatocytes. SOJ Biochemistry. 2017; 2: 6-11.

Babele PK, Thakre PK, Kumawat R, Tomar RS. Zinc oxide nanoparticles induce toxicity by affecting cell wall integrity pathway, mitochondrial function and lipid homeostasis in *Saccharomyces cerevisiae*. Chemosphere. 2018; 213: 65-75.

Blaise C, Gagné F, Harwood M, Quinn B, Hanana H. Ecotoxicity responses of the freshwater cnidarian *Hydra attenuata* to 11 rare earth elements. Ecotoxicol Environ Saf. 2018; 163: 486-491.

Browne MA, Crump P, Niven SJ, Teuten E, Tonkin A, Galloway T, Thompson R. Accumulation of microplastic on shorelines woldwide: sources and sinks. Environ Sci Technol. 2011; 45: 9175-9179.

Bradford MM. A rapid and sensitive method for the quantitation of microgram quantities of protein utilizing the principle of protein-dye binding. Anal Biochem. 1976; 72: 248-254.

Carpenter EJ, Smith KL. Plastics on the Sargasso sea surface. Science 1972; 175: 1240-1241.

DaCosta JP, Santos PSM, Duarte AC, Racha-Santos T. Review: (Nano)plastics in the environment - Sources, fates and effects. STOTEN. 2016; 566-567: 15-26.

Cui R, Kim SW, An Y-J. Polystyrene nanoplastics inhibit reproduction and induce abnormal embryonic development in the freshwater crustacean *Daphnia galeata* Scientific Reports. 2017; 7: 12095.

Erni-Cassola G, Gibson MI, Thompson RC, Christie-Oleza JA. Lost, but found with Nile Red: a novel method for detecting and quantifying small microplastics (1 mm to 20 μm) in environmental samples. Environ Sci Technol. 2017; 51 : 13641-13648.

Fuertes I, Jordao R, Casas J, Barata C. Allocation of glycerolipids and glycerophospholipids from adults to eggs in *Daphnia magna*: Perturbations by compounds that enhance lipid droplet accumulation. Environ Poll. 2018; 242: 1702-1710.

Gagné F, André C, Auclair J, Gagnon C, Turcotte P. The influence of microplastic and nanoparticles of environmental interest on the H2O2-KSCN-CuSO4-NaOH oscillator-implications for ecotoxicology. J Anal Toxicol Appl. 2018;1: 1-6.

Gagné, F. Detection of polystyrene nanoplastics in biological tissues with a fluorescent molecular rotor probe. J. of Xenobiotics 2019, 9: 8147.

Gagné, F, Auclair J, André C. Polystyrene nanoparticles induce anisotropic effects in subcellular fraction of the digestive system of freshwater mussels. Currrent Topics Toxicology 2019, 15, 43-49.

Gall SC, Thompson RC. The impact of debris on marine life. Mar Pollut Bull. 2015; 92: 170-179.

Gigault J, Halle A, Beaudrimont M, Pascal P-Y, Gauffre F, Phi T-L, Hadri HE, Grass B, Reynaud S. Current opinion: What is a nanoplastic? Environ Poll. 2018; 235: 1030-1034.

Greenspan P, Mayer EP, Fowler SD. Nile Red: A Selective Fluorescent Stain for Intracellular Lipid Droplets. The J Cell Biol. 1985; 100: 965 973.

Greenspan P, Fowler SD. Spectrofluorometric studies of the lipid probe, Nile red. J Lipid Res. 1985; 26: 781-978.

Jordão R, Garreta E, Campos B, Lemos MFL, Soares AMVM, Tauler R, Barata C. Compounds altering fat storage in Daphnia magna. STOTEN. 2016; 545–546: 127–136.

Lambert S, Wagner M. Characterisation of nanoplastics during the degradation of polystyrene. Chemosphere. 2016; 145: 265-268.

Langhals H, Zgela D, Schlücker T. High performance recycling of polymers by means of their fluorescence lifetimes. Green and Sustainable Chemistry 2014; 4: 144-150.

Lovric J, Cho SJ, Winnink FM, Maysinger D. Unmodified Cadmium Telluride Quantum Dots Induce Reactive Oxygen Species Formation Leading to Multiple Organelle Damage and Cell Death. Chemistry and Biology. 2005; 12: 1227-1234.

Luo YJ, Wang LH, Chen WNU, Peng SE, Tzen JT-C, Hsiao YY, Huang HJ, Fang LS, Chen CS. Ratiometric imaging of gastrodermal lipid bodies in coral–dinoflagellate endosymbiosis. Coral Reefs 2009; 28: 289–301.

Maes T, Jessop R, Wellner N, Haupt K, Mayes AG. A rapid-screening approach to detect and quantify microplastics based on fluorescent tagging with Nile Red. Scientific Reports. 2017; 7 **:** 44501.

Magni S, Gagné F, André A., Torre CD, Auclair J, Hanana H, Parenti CC, Bonasoro F, Binelli A. Evaluation of uptake and chronic toxicity of virgin polystyrene microbeads in freshwater zebra mussel Dreissena polymorpha (Mollusca: Bivalvia). STOTEN. 2018; 631–632: 778–788.

Murphy F, Quinn B. The effects of microplastic on freshwater Hydra attenuata feeding, morphology & reproduction. Environ Poll. 2018; 234: 487-494.

Quinn, B., Murphy, F., Ewins, C. Validation of density separation for the rapid recovery of microplastics from sediment. Anal Methods. 2016; 9: 1491-1498.

Ribeiro F, Garcia AR, Pereira BP, Fonseca M, Mestre NC, Fonseca TG, Ilharco LM, Bebianno MJ. Microplastics effects in Scrobicularia plana. Marine Poll Bull. 2017; 122: 379–391.

Rist S, Baun A, Hartmann NB. Ingestion of micro- and nanoplastics in Daphnia magna. Quantification of body burdens and assessment of feeding rates and reproduction. Environ Poll. 2017; 228: 398-407.

Shim WJ, Song YK, Hong SH, Jang M. Identification and quantification of microplastics using Nile Red staining. Mar Poll Bull. 2016; 113: 469–476.

Smith M, Love DC, Rochman CM, Neff RA. Microplastics in Seafood and the Implications for Human Health. Curr Environ Health Rep. 2018; 5: 375–386.

Van Sebille E., Plastic in the world's oceans. Sci. Educ. News. 2014; 63: 39-41.

A

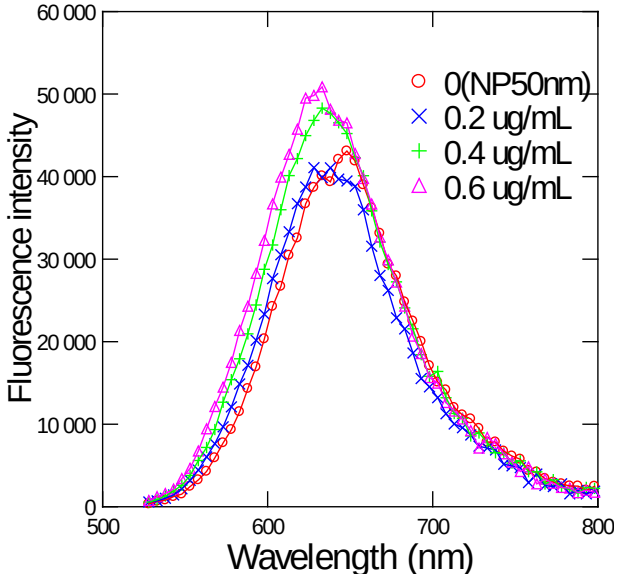
60 000
50 000
40 000
30 000
20 000
10 000
0
500
600
700
800
Fluorescence intensity
Wavelength (nm)
0(NP50nm)
0.2 ug/mL
0.4 ug/mL
0.6 ug/mL

B

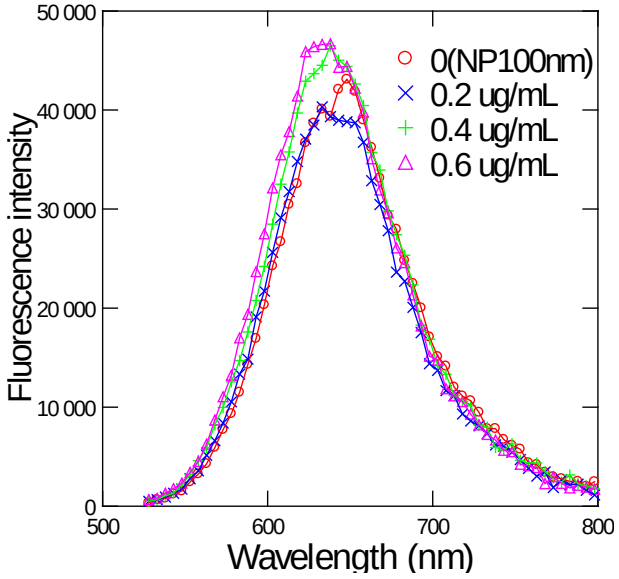
50 000
40 000
30 000
20 000
10 000
0
500
600
700
800
Fluorescence intensity
Wavelength (nm)
0(NP100nm)
0.2 ug/mL
0.4 ug/mL
0.6 ug/mL

C

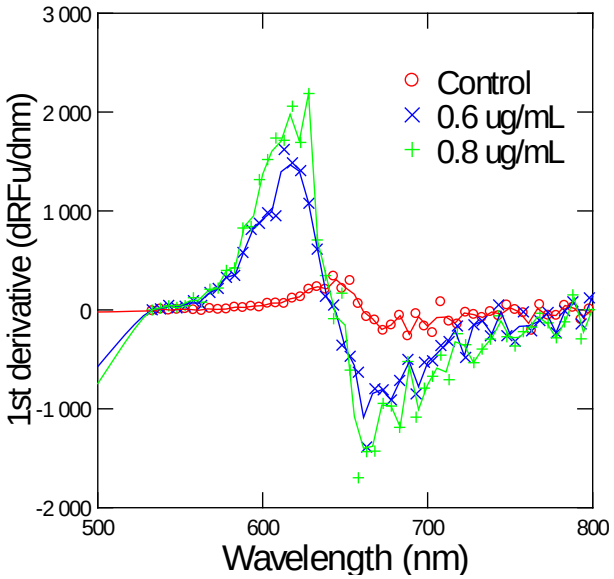

Figure 1. Emission spectra of NR in the presence of increasing amount of NP in subcellular extract. The emission spectra were taken at 500 nm excitation between 530-800 nm. Increasing concentrations of 50 nm (A) and 100 nm (B) were added to a fixed amount of subcellular extract (0.15 mg/mL total protein) and the emission spectra analysed. The first derivative of the fluorescence spectra of 50 nm NPs is shown (C).

A

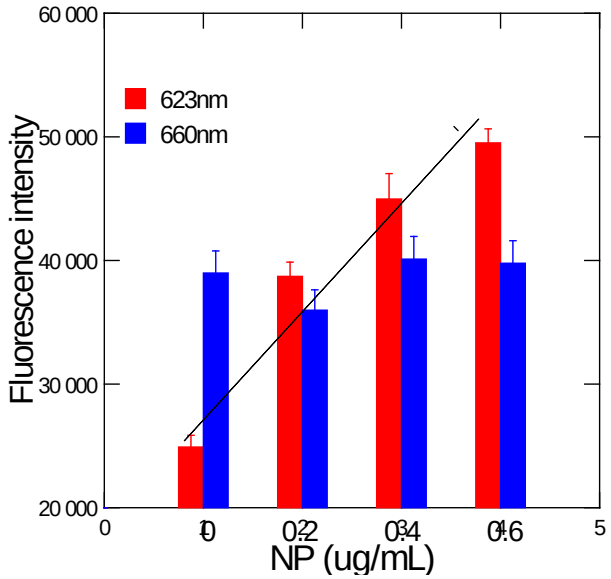

B

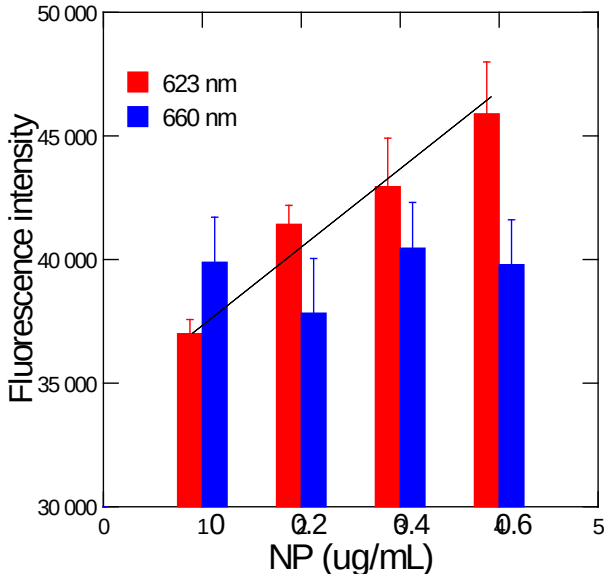

Figure 2. Relationship between NP concentration and Nile Red fluorescence in tissue extracts.

Nile fluorescence was determined in tissue extracts (15 000 x g supernatant) with increasing concentration of polystyrene NP at 50 nm (A) and 100 nm (B) diameter. Fluorescence value at 623 nm corresponds to the changes induced by NP while fluorescence at 660 nm corresponds to lipids in the tissue fraction. A significant linear relationship was obtained for NP 50 nm ($r=0.95$; $p<0.001$; $y = 27500 + 40000x$) and NP 100 nm ($r=0.9$; $p<0.001$; $y= 37585+14092x$).

A

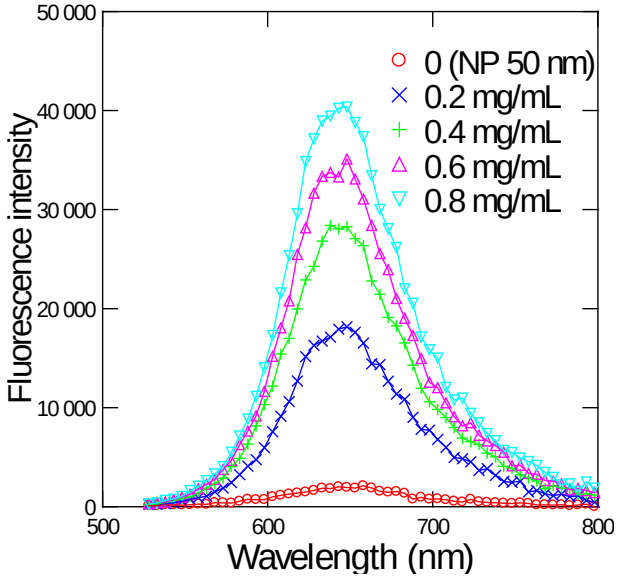
50 000
40 000
30 000
20 000
10 000
0
500
600
700
800
Fluorescence intensity
Wavelength (nm)
0 (NP 50 nm)
0.2 mg/mL
0.4 mg/mL
0.6 mg/mL
0.8 mg/mL

B

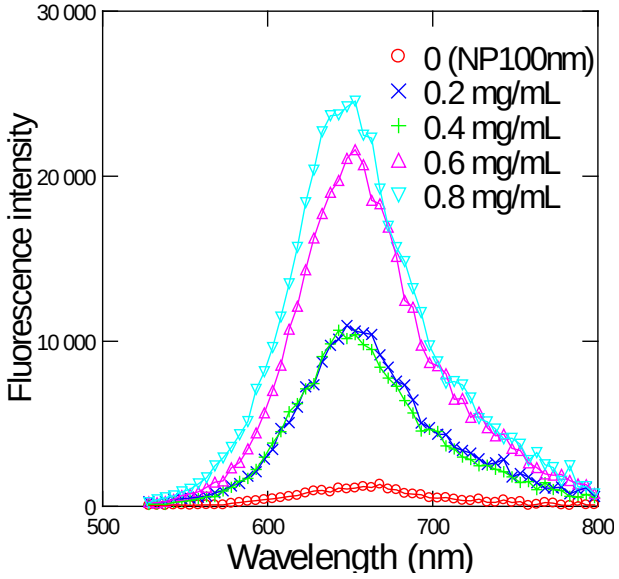
30 000
20 000
10 000
0
500
600
700
800
Fluorescence intensity
Wavelength (nm)
0 (NP100nm)
0.2 mg/mL
0.4 mg/mL
0.6 mg/mL
0.8 mg/mL

…..figure 3

C

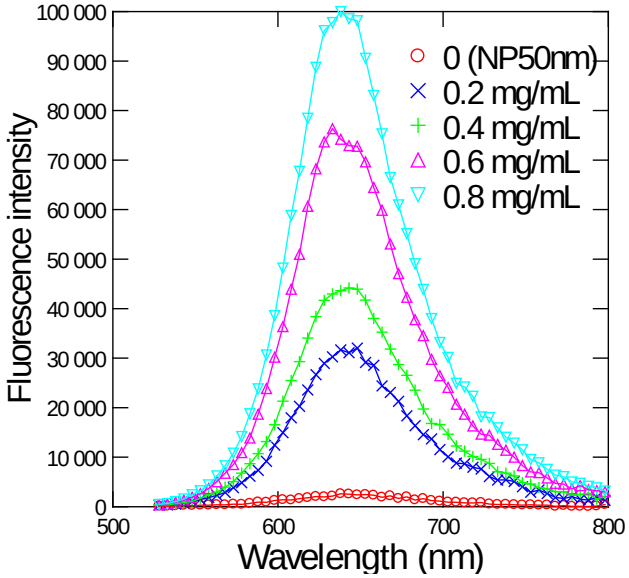

D

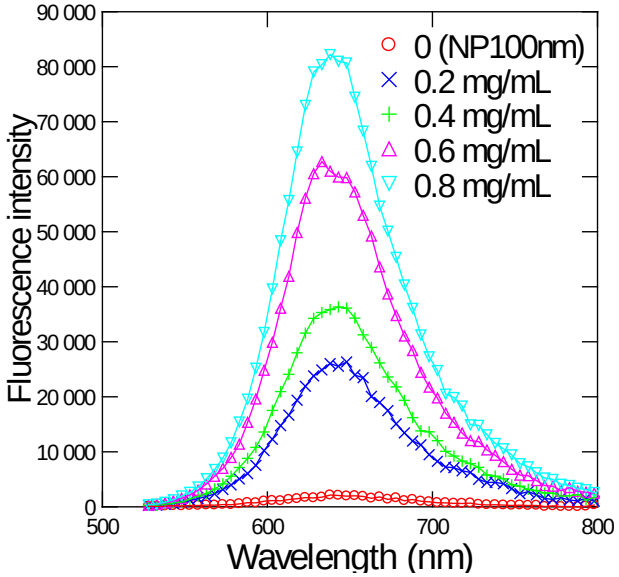

Figure 3. Fluorescence spectra of NP in the presence Nile Red and detergents. Increasing concentration of detergents were added to a fixed 50 nm and 100 nm NP quantity (1 µg/mL). The concentrations of each detergents are indicated in the insert in each emission scans. The emission spectra was taken with 50 nm (A) and 100 nm NP (B) in triton X-100 and with 50 nm (C) and 100 nm (D) in tween-20.

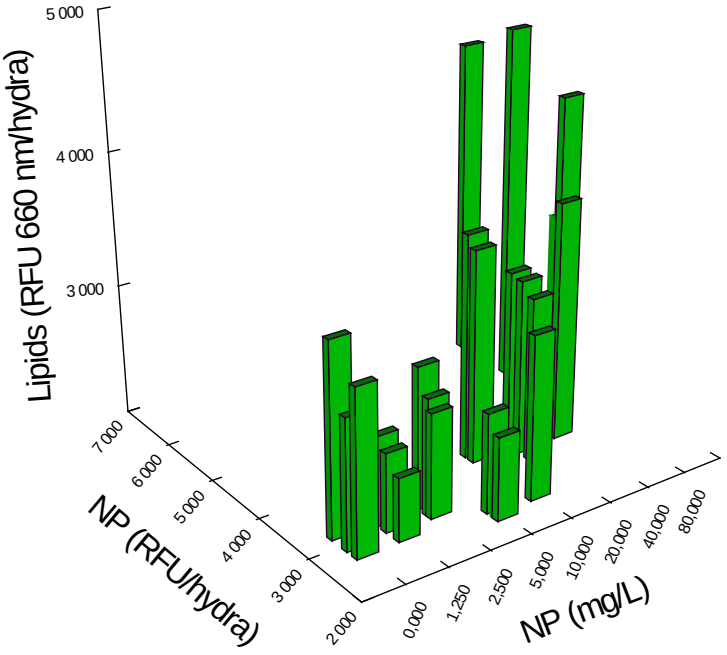

Figure 4. Distribution of Nile red fluorescence in Hydra exposed to 50 nm polystyrene NP. Hydra were exposed to increasing concentration of NP 50 nm for 96 h at 22°C. The Hydra were collected and homogenized in 50 mM NaCl, 25 mM Hepes-NaOH, pH 7.4, and 0.1 mM DTT. RFU: relative fluorescence units.